COMPENSATION OF HEAD-ON BEAM-BEAM INDUCED RESONANCE DRIVING TERMS AND TUNE SPREAD IN RHIC*†

W. Fischer‡, X. Gu, C. Liu, Y. Luo, A. Marusic, R. Michnoff, T.A. Miller, M. Minty,
C. Montag, A.I. Pikin, G. Robert-Demonlaize, V. Schoefer, and P. Thieberger,
Brookhaven National Laboratory, Upton, NY 11973, USA
S.M. White, European Synchrotron Radiation Facility, BP 220, 38043 Grenoble Cedex, France

Abstract

A head-on beam-beam compensation scheme was implemented for operation in the Relativistic Heavy Ion Collider (RHIC) at Brookhaven National Laboratory. The compensation consists of a lattice for the minimization of beam-beam driven resonance driving terms, and electron lenses for the reduction of the beam-beam induced tune spread. We describe the implementations of the lattice and electron lenses, and report on measurements of lattice properties and the effect of the electron lenses on the hadron beam.

INTRODUCTION

In Ref. [1] the implementation of operational head-on beam-beam compensation in RHIC is summarized, consisting of electron lenses (Table 1) for the reduction of the beam-beam induced tune spread, and a lattice for the minimization of resonance driving terms (RDTs). Here we present the lattice design and verification, and measurements of the effect of the electron lenses on tune distribution width. Reference [1] provides references to the only previous attempt at operational beam-beam compensation in DCI [2] as well as the development of the electron lens technology [3] and use in the Tevatron [4]. Details of the RHIC electron lens technology are given in Refs. [5, 6] and references therein. The beam-beam compensation scheme of lattice and lens almost doubled the luminosity, where the lattice alone accounted for about 2/3 of the luminosity increase [1, 7].

For equal normalized rms emittances ϵ_n in all transverse planes, the beam-beam parameter for proton-proton collisions is $\xi_p = -(r_p N_p)/(4\pi\epsilon_n)$, where r_p is the classical proton radius, N_p the bunch intensity, and $\epsilon_n = (\beta_p\gamma_p)\sigma_p^2/\beta$. $(\beta_p\gamma_p)$ are the relativistic factors of the proton beam, σ_p is the rms beam size and β the lattice function.

In RHIC the compensation is implemented in a single turn for one of the two head-on beam-beam interactions [1, 8]. For exact compensation two conditions need to be fulfilled: (i) The correction element is placed at a phase advance of $k\pi$, k being an integer, after the beam- beam interaction in order to minimize the beam-beam RDTs; (ii) a Gaussian electron beam profile of the same width as the proton beam, $\sigma_e = \sigma_p$, and a matching current of $I_e = \left(\frac{N_p}{L_e}\right)\frac{e\beta_e c}{1+\beta_e}$, where β_e is the relativistic factor of the electrons in the lens. The beam-beam parameters from the proton-proton and proton-electron collisions are then $\xi_p = -\xi_e$.

Table 1: Typical Electron Lens Parameters for 2015 (100 GeV Proton Energy) and Design Values (for up to 250 GeV) [1]

quantity	unit	2015	design
distance of center from IP10	m	— 3.3 —	
magnetic length L_e	m	— 2.4 —	
gun solenoid field B_g	T	0.31	≤ 0.69
main solenoid field B_m	T	5.0	2 – 6
cathode radius (2.7σ)	mm	7.5	4.1, 7.5
rms beam size in main solenoid σ_e	μm	650	≥ 300
relativistic factor β_e	...	0.14	≤ 0.2
electron beam current I_e	mA	600	≤ 1000
beam-beam parameter from lens ξ_e	0.001	+10	≤ +15

LATTICE DESIGN AND VERIFICATION

The lattice requires implementation of the phase condition (i) between IP8 and the electron lenses near IP10. In addition, a transversely large proton beam at the location of the lens makes alignment of the two beams easier, and suppresses instabilities driven by the electron-proton beam interaction in the electron lens [9]. As long as the lattice tune is away from a low order resonance, the colliding proton beam lifetime is limited by the beam-beam interaction and the off-momentum dynamic aperture [10]. An effort was made to also reduce the nonlinear chromaticity in order to increased off-momentum dynamic aperture [11].

For a squeezed optics, the β-functions at the final focusing quadrupoles are significantly increased and give rise to chromatic aberrations. An option for a passive correction of these aberrations is the ATS optics [12]. It uses a β-beat wave propagating through the arcs and low-β insertions to further reduce the β-function at the IP without changing the chromatic properties of the lattice.

Figure 1 shows the ATS lattice for the RHIC Blue ring. The β-beat wave is launched in IR4 and closed in IR10. The phase advance and final β-function at the electron lenses are set during the ATS squeeze. It was possible to exactly match the phase advance $\Delta\psi_{x,y} = k\pi$ and increase the β-function at the electron lens to 15 m. The Yellow ring features similar properties. As shown in Fig. 2 the non-linear chromaticity of the 2015 ATS lattices is equal to or smaller than the one of the 2012 lattices for all planes but the Blue vertical one.

The linear lattice functions were measured with a small kick and observing the resulting free betatron oscillations

* Work supported by Brookhaven Science Associates, LLC under Contract No. DE-AC02-98CH10886 with the U.S. Department of Energy.
† This article is an abridged version of a paper submitted to Physical Review Accelerators and Beams.
‡ Wolfram.Fischer@bnl.gov

ISBN 978-3-95450-182-3

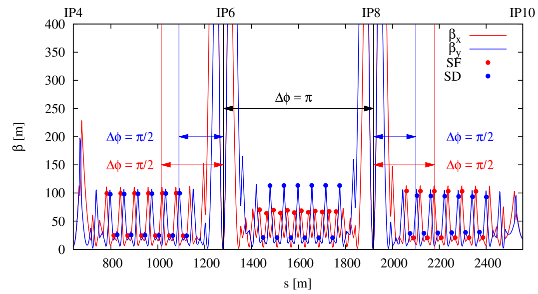

Figure 1: RHIC Blue ring ATS lattice for 100 GeV protons. Only a fraction of the 3.8 km circumference is shown.

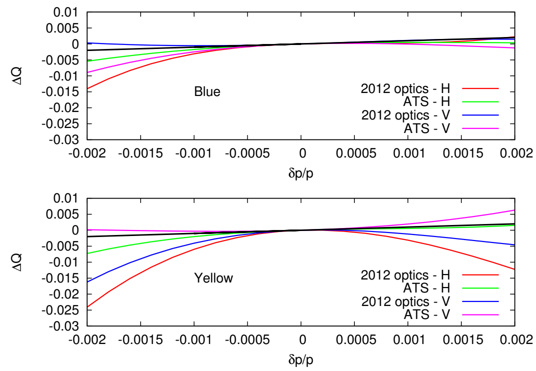

Figure 2: Blue (top) and Yellow (bottom) non-linear tune dependence on the momentum deviation $\delta p/p$ for the 2012 lattice and the 2015 ATS optics. The black line in both plots corresponds to a linear chromaticity $Q' = +1$.

with beam position monitors (BPMs). In Table 2 the model and measured β-functions and phase advances $\Delta\psi_{x,y}$ are listed. A large β-beat will reduce the effectiveness of the ATS lattice in compensating resonance driving terms. Measurements of the β-beat are shown in Fig. 3.

Table 2: Design and Measured Lattice Functions

quantity	unit	design	meas. (B)	meas. (Y)
β_x/β_y at IP6	m	0.85/0.85	0.76/0.78	0.90/0.95
β_x/β_y at IP8	m	0.85/0.85	0.90/0.84	0.88/0.82
β_x/β_y at e-lens	m	15.0/15.0	15.8/14.1	16.5/12.6
$\Delta\psi_x/\Delta\psi_y$ IP8 to lens	deg	180/180	184/177	192/180
$(\Delta\beta/\beta)_x/(\Delta\beta/\beta)_y$	%	11.7/12.1	0/0	11.7/14.1
$\frac{1}{2}Q''_x/\frac{1}{2}Q''_y$ (B)	...	−600/−1350	−400/−1400	
$\frac{1}{2}Q''_x/\frac{1}{2}Q''_y$ (Y)	...	−800/−850		−50/−1200

The nonlinear chromaticity was measured by observing the tune change with a 1.25 mm radius excursion. The results of this measurement are also listed in Table 2. The agreement between design and measured Q'' is good in the Blue ring, and significantly off for the Yellow horizontal plane.

EFFECT OF THE ELECTRON LENSES ON TUNE SPREAD

To measure the tune distributions width, Beam Transfer Functions (BTFs) were used. These measure the complex beam response $R(Q)$ of a small harmonic dipole oscillation of variable frequency $2\pi Q$. A non-zero particle distribution at tune Q is given if $\mathrm{Im}(R) > 0$ [13, 14].

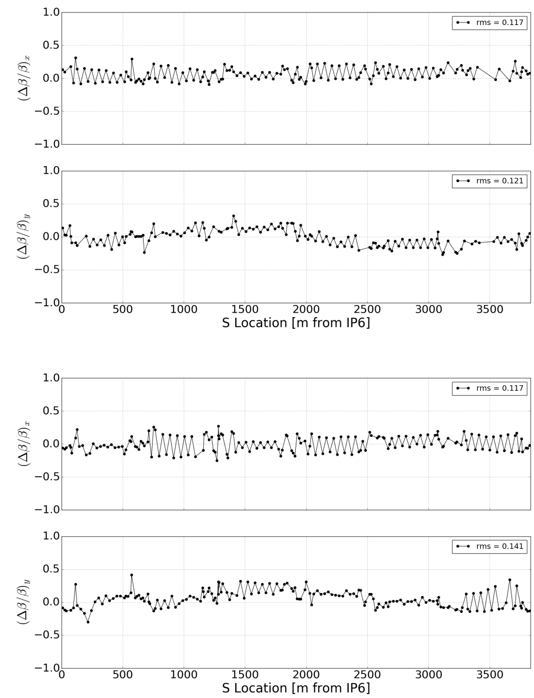

Figure 3: Measured $\Delta\beta/\beta$ for the Blue (top) and Yellow (bottom) horizontal and vertical planes.

With the operational tunes in p+p operation coherent beam-beam modes are excited in a BTF measurement, and the tune distribution widths could not be extracted although this was possible in simulations [14]. To obtain the incoherent tune distribution widths with colliding beams, BTF measurements were done in p+Al collisions. Al beams have fractional tunes near 0.225 and p beams near 0.69. The tune separation is large enough to suppress coherent beam-beam modes. Figure 4 shows the incoherent tune distribution width as a function of the electron beam current I_e for a constant electron beam size of $\sigma_e = 0.55$ mm. Figure 5 shows the tune distributions as a function of the electron beam size σ_e with an electron beam current $I_e = 900$ mA.

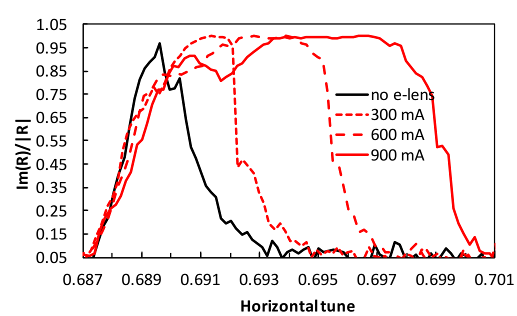

Figure 4: Measured p beam tune distribution width as a function of I_e without beam-beam collisions and with $\sigma_e = 0.55$ mm. Curves are aligned to the left [1].

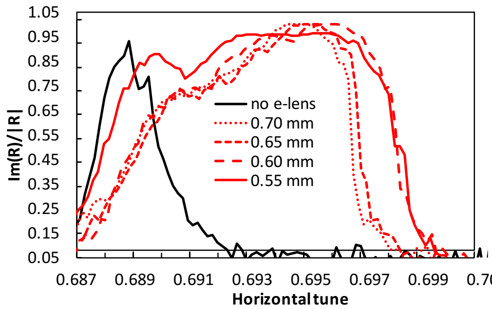

Figure 5: Measured p beam tune distribution width as a function of σ_e with I_e = 900 mA.

If the beam-beam generated tune shift at amplitude a is denoted by $\delta Q_{p,e}(a)$, the generated tune spread over the range from zero to a is

$$\Delta Q_{bb}(a) = |\xi_{p,e} - \delta Q_{p,e}(a)|. \tag{1}$$

and the total tune spread ΔQ_{tot} is assumed to be given by

$$\Delta Q^2_{tot} = \Delta Q^2_0 + \Delta Q^2_{bb}(a) \tag{2}$$

where ΔQ_0 is the tune spread without beam-beam.

Figure 6 shows a comparison of the measured increase in the tune distribution width for the current scan shown in Fig. 4 and the beam size scan shown in Fig. 5. The measurement matches the calculation for a fitted value $a = 2.5\,\sigma_e$. There are only few particles at amplitudes $a > 2.5\,\sigma_e$ and the BTF signal R is weak with small particle numbers.

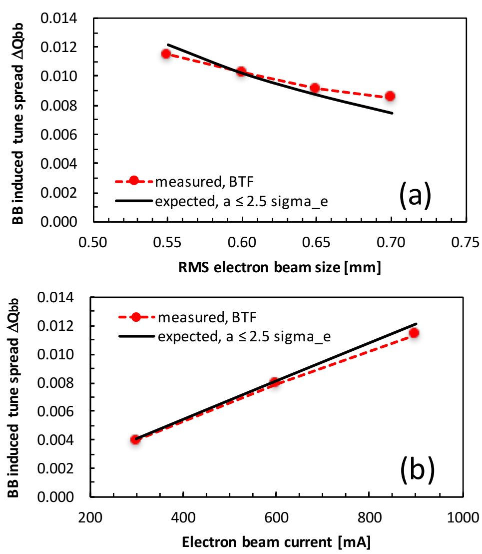

Figure 6: Measured and calculated increase in the tune spread in a σ_e scan (a) and a I_e scan (b). The calculation is for an amplitude range a from zero to 2.5 σ_e.

Finally, Fig. 7 shows the tune distribution width without and with beam-beam interaction, and with an increasing electron beam current (σ_e = 0.65 mm), taken with a p-beam colliding with an Al beam. The tune spread increases with the beam-beam interaction and is gradually compressed with an increasing electron beam current I_e up to the initial tune distribution. A further increase in I_e does not lead to a further reduction in ΔQ_{tot}. The initial tune spread is primarily due to non-zero chromaticity and momentum spread, and cannot be compensated for with the electron lens. For further increasing currents one expects the tune distribution width to widen again.

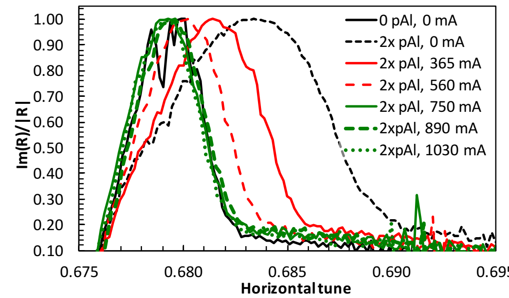

Figure 7: Tune distribution width reduction with the electron lens, measured in the proton beam with p+Al collisions.

Figure 8 shows a comparison between measured and expected ΔQ_{tot} as a function of I_e. The expected value is based on the BTF-measured ΔQ_0 and $\Delta Q_{bb}(a)$ using Eqs. (1) and (2), where $\Delta Q_{bb}(\infty) = |(2\xi_{Al} + \xi_e)|$. The figure shows the expected ΔQ_{tot} for $a \leq 2.5\,\sigma_p$, a good fit in Fig. 6, and for $a \leq 3.5\,\sigma_p$, a better fit in this case.

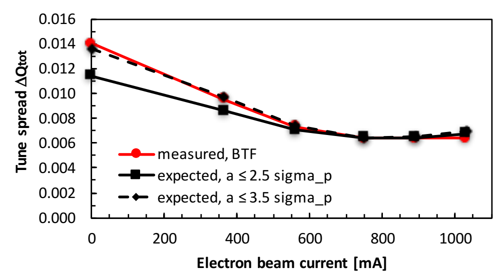

Figure 8: Total tune spread ΔQ_{tot} as a function of the electron beam current I_e.

SUMMARY

For the head-on beam-beam compensation scheme in RHIC a lattice was designed and its properties measured, and β-functions and phase advances are close to the design values. The incoherent tune spread generated by the electron lenses was measured and is in agreement with BTF based measurements of the tune spread, assuming that particles in the amplitude range from zero to 2.5 σ_e are detected in the measurement. The beam-beam generated tune spread is indeed compensated by the electron lens.

ACKNOWLEDGMENTS

We are thankful to the C-AD and SMD groups at BNL. We are also grateful to V. Shiltsev, A. Valishev, T. Sen, and G. Stancari, FNAL; N. Milas, ESS; X. Buffat, R. DeMaria, U. Dorda, W. Herr, J.-P. Koutchouk, T. Pieloni, F. Schmidt, and F. Zimmerman, CERN; K. Ohmi, KEK; J. Qiang, LBNL; V. Kamerdziev, FZ Jülich; A. Kabel, SLAC and P. Görgen, TU Darmstadt. The US LHC Accelerator Research Program (LARP) supported beam-beam simulations.

REFERENCES

[1] W. Fischer et al., PRL 115, 264801 (2015).

[2] M. Bergher et al., "Status report on D.C.I.", in Proc. PAC'79; IEEE Trans Nucl. Sci. NS-26, 3559-3561, 1979.

[3] V. Shiltsev, Electron Lenses for Super-Colliders, Springer, New York, Heidelberg, Dordrecht, London, 2016.

[4] V. Shiltsev et al., Phys. Rev. Lett., vol. 99, p. 244801, 2007.

[5] P. Thieberger et al., "High Energy Coulomb-Scattered Electrons for Relativistic Particle Beam Diagnostics", Phys. Rev. AB, vol. 19, p. 041002, 2016.

[6] X. Gu et al., "Electron Lenses for Head-On Beam-Beam Compensation in RHIC", Phys. Rev. AB, vol. 20, p. 023501, 2017.

[7] V. Schoefer et al., "RHIC polarized proton-proton Operation at 100 GeV in Run 15", in Proc. IPAC'15, pp. 2384-2386, 2015.

[8] Y. Luo et al., "Six-Dimensional Weak-Strong Simulation of Head-On Beam-Beam Compensation in the Relativistic Heavy Ion Collider", Phys. Rev. ST:AB, vol. 15, p. 051004, 2012.

[9] A. Burov, V. Danilov, and V. Shiltsev, "Transverse Beam Stability with an Electron Lens", Phys. Rev. E, vol. 59, p. 3605, 1999.

[10] Y. Luo, W. Fischer, and S. White, "Analysis and Modeling of Proton Beam Loss and Emittance Growth in the Relativistic Heavy Ion Collider", Phys. Rev. AB, vol. 19, p. 021001, 2016.

[11] S. White, W. Fischer, and Y. Luo, "Optics Solutions for pp Operation with Electron Lenses at 100 GeV", BNL-105550-2014-IR, C-A/AP/519, 2014.

[12] S. Fartoukh, "Achromatic Telescopic Squeezing Scheme and Application to the LHC and its Luminosity Upgrade", Phys. Rev. ST:AB, vol. 16, p. 111002, 2013.

[13] A.W. Chao, Physics of Collective Beam Instabilities in High Energy Accelerators, John Wiley & Sons., New York, Chichester, Brisbane, Toronto, Singapore, Chapter 5, 1993.

[14] P. Görgen, O. Boine-Frankenheim, and W. Fischer, "Beam Transfer Functions for Relativistic Proton Bunches with Beam-Beam Interactions", NIM A 777, pp. 43-53, 2015.